(2)

AD-A195 800

REPORT DOCUMENTATION PAGE

1b. RESTRICTIVE MARKINGS

2a. SECURITY CLASSIFICATION AUTHORITY

3. DISTRIBUTION/AVAILABILITY OF REPORT
Approved for Public Release
Distribution is Unlimited

2b. DECLASSIFICATION/DOWNGRADING SCHEDULE
NA

4. PERFORMING ORGANIZATION REPORT NUMBER(S)
None

5. MONITORING ORGANIZATION REPORT NUMBER(S)
AFOSR-TR- 88-0469

6a. NAME OF PERFORMING ORGANIZATION
Pennsylvania State University

6b. OFFICE SYMBOL (If applicable)

7a. NAME OF MONITORING ORGANIZATION
AFOSR

6c. ADDRESS (City, State and ZIP Code)
Mechanical Engineering Dept.
University Park, PA 16802

7b. ADDRESS (City, State and ZIP Code)
Same as 6c.

8a. NAME OF FUNDING/SPONSORING ORGANIZATION
Air Force Office of Scientific Research

8b. OFFICE SYMBOL (If applicable)
NA

9. PROCUREMENT INSTRUMENT IDENTIFICATION NUMBER
AFOSR-82-0196

8c. ADDRESS (City, State and ZIP Code)
B199 410
Bolling AFB, Washington, D.C. 20332

10. SOURCE OF FUNDING NOS.

PROGRAM ELEMENT NO.	PROJECT NO.	TASK NO.	WORK UNIT NO.
61102F	2308	A1	

11. TITLE (Include Security Classification) Computation of Low Speed Compressible Flows with Time-Marching Procedures

12. PERSONAL AUTHOR(S)
Charles L. Merkle and Yun-Ho Choi

13a. TYPE OF REPORT	13b. TIME COVERED	14. DATE OF REPORT (Yr., Mo., Day)	15. PAGE COUNT
Article	FROM _____ TO _____		38

16. SUPPLEMENTARY NOTATION

17. COSATI CODES			18. SUBJECT TERMS (Continue on reverse if necessary and identify by block number)
FIELD	GROUP	SUB. GR.	

19. ABSTRACT (Continue on reverse if necessary and identify by block number)

The extension of time-marching procedures to low Mach number and low Reynolds number conditions is considered. It is shown that the disparate speeds of the acoustic and particle waves prevents convergence at high Reynolds numbers while the requirement that both the Courant and the von Neumann numbers be of order one prevents convergence in very viscous flows. A perturbation expansion is used to introduce pseudo-acoustic waves that propagate at speeds similar to the particle speed at high Reynolds numbers and that allows both the inviscid and viscous time step parameters to be of order one at low Reynolds numbers. The resulting algorithm is shown to give convergence rates that are independent of either Mach number or Reynolds number over a range of five orders of magnitude in both parameters. Results are shown for strong heat addition in low speed flow encompassing this broad range of variables.

20. DISTRIBUTION/AVAILABILITY OF ABSTRACT
UNCLASSIFIED/UNLIMITED ☒ SAME AS RPT. ☑ DTIC USERS ☐

21. ABSTRACT SECURITY CLASSIFICATION
Unclassified

22a. NAME OF RESPONSIBLE INDIVIDUAL	22b. TELEPHONE NUMBER (Include Area Code)	22c. OFFICE SYMBOL
Dr. Mithat Birkan	(202) 767-4938	AFOSR/NA

DD FORM 1473, 83 APR EDITION OF 1 JAN 73 IS OBSOLETE.

SECURITY CLASSIFICATION OF THIS PAGE
UNCLASSIFIED

COMPUTATION OF LOW-SPEED COMPRESSIBLE FLOWS WITH TIME-MARCHING PROCEDURES

Charles L. Merkle and Yun-Ho Choi
The Pennsylvania State University
Department of Mechanical Engineering
214 Mechanical Engineering Building
University Park, Pennsylvania 16802

ABSTRACT

The extension of time-marching procedures to low Mach number and low Reynolds number conditions is considered. It is shown that the disparate speeds of the acoustic and particle waves prevents convergence at high Reynolds numbers while the requirement that both the Courant and the von Neumann numbers be of order one prevents convergence in very viscous flows. A perturbation expansion is used to introduce pseudo-acoustic waves that propagate at speeds similar to the particle speed at high Reynolds numbers and that allows both the inviscid and viscous time step parameters to be of order one at low Reynolds numbers. The resulting algorithm is shown to give convergence rates that are independent of either Mach number or Reynolds number over a range of five orders of magnitude in both parameters. Results are shown for strong heat addition in low speed flow encompassing this broad range of variables.

INTRODUCTION

Time-dependent algorithms are nearly the exclusive choice for the computation of compressible flows. They have been highly developed to apply to high speed flows in general, and to deal with the shock waves that frequently appear under such conditions, in particular. Both explicit and implicit procedures have been used extensively in transonic, supersonic, and hypersonic regimes. An important advantage of these algorithms is that they provide accurate predictions in both inviscid flows and in the practically important regime of high Reynolds number viscous flows. One reason for this flexibility is that they allow the convective terms to be central differenced at all Reynolds numbers. In cases where central differences are not desired, they provide a physical

basis for defining various upwind differencing schemes also. In general, upwind differencing becomes more desirable as the Mach number increases.

An important attribute of any computational algorithm is that it be robust over a wide range of flow conditions. In this regard, a major drawback of time-dependent procedures is their well-known inefficiency at low subsonic speeds. This characteristic can lead to difficulties in computations of transonic flowfields that contain embedded low speed regions such as near a stagnation point or in the boundary layer. In addition, this limitation makes the family of algorithms ineffective for computing combustion problems in which the velocities are generally low, but where the flowfields remain strongly compressible because of heat release. An additional low speed, compressible flow problem that is of interest to the present authors is the interaction between high intensity radiation fields, including both high power laser beams and focussed solar radiation, and flowing gases[1,2]. Our purpose in the present paper is to identify the reasons why these time-dependent algorithms fail at low speeds and to devise methods for enhancing convergence in these regimes so that they can be used effectively for these additional applications.

In addition to extending time-marching methods to low speed applications, a second motive for studying this problem is to enable us to understand their convergence characteristics more thoroughly. Besides increasing the range of convergence, this improved understanding may also point the way toward improving the convergence rate in those regions where the methods are already applicable. In the present paper, we study the characteristics of time-marching algorithms in this light. We address the primary question of how these popular algorithms can be

extended to low Mach number, low Reynolds number flows. Throughout our attention is limited to steady flows.

Methods for enhancing low Mach number convergence in inviscid flows have been considered by several previous authors[3-9], but no one has as yet addressed the viscous problem. In the present paper, we first review this previous work in inviscid flows and then extend these procedures to the viscous case. Our analysis is based upon implicit algorithms that use central differencing in space. The Mach-number/Reynolds-number regime we consider ranges from high subsonic speeds (Mach numbers of about 0.1) down to incompressible speeds (Mach numbers around 10^{-6}) and from inviscid flow (infinite Reynolds numbers) down to highly viscous conditions (Reynolds numbers less than unity). Appropriate modifications to the implicit algorithm are made that allow a single unified procedure to give efficient convergence over this entire range. Although testing with explicit algorithms has not been attempted, it is presumed that these procedures will also provide similar improvements in convergence for explicit schemes over this wide regime. The philosophies used here should also prove useful for developing efficient convergence of flux-split schemes that use upwind differencing.

REVIEW OF CONVERGENCE ENHANCEMENT IN INVISCID LOW MACH NUMBER FLOWS

The convergence rate of traditional time-dependent algorithms for inviscid flows slows down as the Mach number is reduced because of the increasing diversity of the speeds of the eigenvalues. As these eigenvalues become stiff, both explicit and implicit algorithms show slower convergence for distinct, but related, reasons. Explicit schemes slow down because the maximum allowable time-step is strictly limited by

stability considerations and the CFL corresponding to the slower eigenvalues approaches zero. Implicit approximately-factored algorithms slow down because the factorization introduces an optimum CFL. Slower convergence is observed for CFL's above or below this optimum. When the Mach number is low, only one of the eigenvalues (say, for example, the u or u+c eigenvalue) can be kept at a CFL near this optimum while the others are far from the optimum and convergence slows dramatically. As is shown later, fully implicit algorithms that use direct inversion of the complete multidimensional matrix (no approximate factorization) do not show a convergence slowdown because of eigenvalue stiffness. They continue to show rapid convergence rates that are independent of Mach number. The reason for this is because direct inversion methods do not exhibit an optimum CFL, but continue to converge more rapidly as CFL is increased.

There have been two distinct methods proposed for circumventing the convergence slowdown induced by eigenvalue stiffness. One method is to use time-derivative preconditioning. Early studies[3-5] of preconditioning showed that rapid convergence could be achieved down to Mach numbers of about 0.01. More recently, we have shown[10] that preconditioning allows Mach-number-independent convergence down to Mach numbers of 10^{-5}, but that round-off errors begin to affect the maximum convergence level at Mach numbers below 10^{-3}. In this regard it is notable that it is round-off errors in the pressure (not density as might be expected) that eventually prohibits the use of the preconditioned approach.

The second method for circumventing low Mach number convergence difficulties has been through using special perturbed forms of the equations of motion that are valid at low Mach numbers. Gustafsson[6] has

used an expansion in Mach number while the present authors[8] have used an expansion in Mach number squared. Gustafsson's philosophy was to symmetrize the matrices corresponding to the Jacobians of the flux vectors. Our Mach number squared expansion was used to control the disparity in the eigenvalues and left the matrices non-symmetric. Our numerical results showed effective convergence control to Mach numbers of 10^{-6}. Calculations at lower Mach numbers were not attempted, but we estimate flows to 10^{-8} or 10^{-10} in Mach number could be computed before unacceptable round-off error would begin to decimate the results. Although we are not aware of similar tests of Gustafsson's expansion procedure, our interpretation of his approach suggests that it would also be effective in providing Mach-number-independent convergence rates.

Extension of these low Mach number methods to viscous flows has heretofore not been attempted. The purpose of the present paper is to develop a method that allows rapid convergence over all Reynolds number regimes without sacrificing convergence rate in the inviscid case. The procedure described here is based upon the perturbation expansion procedure.

THE CHOICE OF A REPRESENTATIVE PROBLEM

We are interested in assessing the convergence rate of numerical algorithms over a broad Reynolds-number/Mach-number spectrum ranging from inviscid to highly viscous conditions and from high subsonic speeds to very low velocities. To make this assessment we need a representative problem that will possess a non-trivial solution over the entire Reynolds-Mach number regime. As such a problem we choose the flow through a duct with volumetric heat addition (Fig. 1). The heat addition causes large density changes such that even in the presence of low

velocities, the compressible form of the equations must be used. This problem is representative of typical combustion problems, and is also analogous to the radiation/gasdynamic interactions[1,2] mentioned above.

In the absence of viscous effects, the presence of a spatially varying volumetric heat source prevents the solution from being a trivial, uniform flow and instead generates an inviscid flowfield that is strongly two-dimensional. When the effects of viscosity are included, the no-slip condition on the wall ensures that the velocity profiles will be non-uniform. At very low Reynolds number, however, fully developed conditions are rapidly established and the introduction of a heat source again provides a more general flowfield at either low or high Reynolds numbers. For viscous flows we use both volumetric heat sources and heat addition through the walls.

CONVERGENCE OF THE TRADITIONAL TIME-DEPENDENT PROCEDURE

As a first assessment of the problem, we report the convergence rate of a traditional approximately-factored scheme with no provision for low Reynolds number or low Mach number. In their standard form the equations are:

$$\frac{\partial Q}{\partial t} + \frac{\partial E}{\partial x} + \frac{\partial F}{\partial y} = \frac{\partial}{\partial x}\left(V_{xx} + V_{xy}\right) + \frac{\partial}{\partial y}\left(V_{yx} + V_{yy}\right) \qquad (1)$$

where the vectors Q, E, F, V_{xx}, V_{xy}, V_{yx} and V_{yy} are:

$$Q = \begin{pmatrix} \rho \\ \rho u \\ \rho v \\ e \end{pmatrix} \quad E = \begin{pmatrix} \rho u \\ \rho u^2 + p \\ \rho uv \\ (e+p)u \end{pmatrix} \quad F = \begin{pmatrix} \rho v \\ \rho uv \\ \rho v^2 + p \\ (e+p)v \end{pmatrix} \qquad (2)$$

∂ = partial differential; ρ = rho

$$V_{xx} = \begin{pmatrix} 0 \\ 4/3\mu\frac{\partial u}{\partial x} \\ \mu\frac{\partial v}{\partial x} \\ k\frac{\partial T}{\partial x} \end{pmatrix} V_{xy} = \begin{pmatrix} 0 \\ -\frac{2}{3}\mu\frac{\partial v}{\partial y} \\ \mu\frac{\partial u}{\partial y} \\ 0 \end{pmatrix} V_{yx} = \begin{pmatrix} 0 \\ \mu\frac{\partial v}{\partial x} \\ \frac{2}{3}\mu\frac{\partial u}{\partial x} \\ 0 \end{pmatrix} \quad V_{yy} = \begin{pmatrix} 0 \\ \mu\frac{\partial u}{\partial y} \\ \frac{4}{3}\mu\frac{\partial v}{\partial y} \\ k\frac{\partial T}{\partial y} \end{pmatrix} \tag{3}$$

Here, p, ρ, u and v are the pressure, density and x and y components of the velocity; e is the total internal energy that is related to the other parameters by $e = \rho[\varepsilon + \frac{1}{2}(u^2 + v^2)]$ where ε is the internal energy. The diffusion terms contain the viscosity, μ, and the thermal conductivity, k. For simplicity, Stokes hypothesis has been used, and in anticipation of low Mach number applications, the viscous dissipation has been dropped. The speed of sound, c, is given as $c^2 = \gamma p/\rho$ where γ is the ratio of specific heats.

Traditional approximately-factored Euler implicit algorithms applied to Eqn. 1 lead to the following[11,12]:

$$\begin{aligned} &(I/\Delta t + \frac{\partial}{\partial x}A - \frac{\partial}{\partial x}R_{xx}\frac{\partial}{\partial x})(I/\Delta t + \frac{\partial}{\partial y}B - \frac{\partial}{\partial y}R_{yy}\frac{\partial}{\partial y})\Delta Q \\ &= -[\frac{\partial E}{\partial x} + \frac{\partial F}{\partial y} - \frac{\partial}{\partial x}(V_{xx} + V_{xy}) - \frac{\partial}{\partial y}(V_{yx} + V_{yy})]^n \end{aligned} \tag{4}$$

where superscripts refer to the time step level, and ΔQ is the change in Q in one time step ($\Delta Q = Q^{n+1} - Q^n$). The matrices R_{xx} and R_{yy} are appropriate Jacobians of V_{xx} and V_{yy}.

The rates of convergence of the classical approximate factorization scheme for the test problem given in Fig. 1 are shown in Fig. 2 for a

---

μ = mu; ε = epsilon; γ = gamma; Δ = delta

wide range of inlet Mach numbers. At high subsonic speeds (0.7 Mach number) the scheme converges rapidly. Convergence to machine accuracy is achieved in some 380 steps. As the Mach number is reduced, the convergence gets much slower as intimated above. At a Mach number of 0.4, the convergence has already slowed down by more than a factor of two, and about 1000 iterations are needed to reach machine accuracy. At Mach 0.1, some 4500 iterations are required, while at a Mach number of 0.01, extrapolation suggests it will take some 45,000 steps to reach machine accuracy. Because of the difficulties in finding optimum convergence rates at such slowly converging conditions, the results shown here were all computed at a CFL (based on u+c) of 6.0. At the lower Mach numbers, somewhat faster convergence could probably have been obtained for slightly different values of CFL, but the rates shown here are within a factor of two of their optimum value. Clearly, the standard procedure is unacceptably inefficient at low speeds.

The physical reason for these convergence difficulties is easily understood. The time-iterative procedure relies upon both acoustic waves and particle trajectories to propagate errors out of the flowfield. At low Mach numbers the acoustic waves make many trips through the flowfield while the particles are traversing it a single time. Approximate factorization provides most rapid convergence when the individual waves move a modest fraction of the distance across the computational domain in a single time step. A CFL of about 5 based on u+c provides this optimum propagation rate for the acoustic waves, but at low Mach numbers the corresponding CFL based on u is so small that the particles move very small distances in one time step and it takes many steps for them to traverse the flowfield. For this reason the above results show that the

number of iterations varies approximately inversely with the Mach number. Other alternative choices of CFL do not provide materially faster convergence.

Proof that it is the approximate factorization errors that cause this slowdown in convergence is easily obtained from either a stability analysis of Eqn. 4, or from its direct solution without approximate factorization. If we define the amplification matrix, G, as

$$(G-I)Q^n = \Delta Q \tag{5}$$

the Fourier transform of Eqn. 4 gives G as the product of two matrices, $G = K_1^{-1}K_2$ where,

$$K_1 = I + i[S_x \frac{\Delta t}{\Delta x}A + S_y \frac{\Delta t}{\Delta y}B] + 2[(1-C_x)\frac{\Delta t}{\Delta x^2} R_{xx} + (1-C_y)\frac{\Delta t}{\Delta y^2} R_{yy}] + T_{AF}$$

$$K_2 = I - S_x S_y \frac{\Delta t}{\Delta x \Delta y} (R_{xy} + R_{yx}) + T_{AF} \tag{6}$$

Here, S_x, C_x, S_y and C_y represent the trigonometric functions of the Fourier modes in the x and y directions, and i is the square root of minus one. The term, T_{AF}, represents the errors introduced by approximate factorization. If the algorithm is solved without factorization, T_{AF} vanishes; if approximate factorization is included, it becomes,

$$T_{AF} = [iS_x \frac{\Delta t}{\Delta x}A + 2(1-C_x)\frac{\Delta t}{\Delta x^2} R_{xx}][iS_y \frac{\Delta t}{\Delta y}B + 2(1-C_y)\frac{\Delta t}{\Delta y^2} R_{yy}] \tag{7}$$

Although these expressions for the amplification matrix are quite involved, numerical eigenvalues are easily found as parametric functions of the Fourier wavenumbers in the x and y directions for specific flow conditions. Contour plots of the maximum eigenvalue of G obtained from Eqn. 6 are given in Fig. 3 for flow conditions that include a Mach number

of 10^{-4} and a Reynolds number of 50. Figure 3a shows the maximum amplification factors at CFL = 6 (based on u+c) for the case with approximate factorization. As can be seen, approximate factorization is stable, but the eigenvalues are near unity everywhere.

The corresponding stability characteristics without approximate factorization ($T_{AF} = 0$) are given in Fig. 3b. Here, we have used a CFL of 21,000 to offset the low Mach number and the amplification rates are much less than unity everywhere suggesting rapid convergence. Numerical experiments with the fully implicit system using direct inversion rather than approximate factorization verify this. In general, they reach machine accuracy in 8 or 9 time steps. Direct-inversion, implicit procedures eliminate convergence difficulties at low Mach numbers and provide a very robust computational algorithm. Unfortunately, the CPU requirements for direct solution are prohibitive for even moderately refined two-dimensional grids and more so for three-dimensional problems, and the procedure is not practical for routine calculations.

LOW MACH NUMBER EXPANSION

To obtain a system of equations that is valid for low speed viscous flows, we use a perturbation expansion similar to that used in Ref. 8 except that here we perturb the non-conservative form of the equations rather than the conservative form. The method developed in Ref. 8 for inviscid flows is unstable at moderate and low Reynolds numbers and cannot be used for viscous flows. When expressed in non-conservative form, the equations are:

$$\frac{\partial \tilde{Q}}{\partial t} + \tilde{A}\,\frac{\partial \tilde{Q}}{\partial x} + \tilde{B}\,\frac{\partial \tilde{Q}}{\partial y} = \frac{1}{\rho}\,\frac{\partial}{\partial x}\,(V_{xx} + V_{xy}) + \frac{1}{\rho}\,\frac{\partial}{\partial y}\,(V_{yx} + V_{yy}) \qquad (8)$$

$\sim$ = equivalent, similar

where $Q = (\rho, u, v, p)^T$ and the Jacobians $\tilde{A}$ and $\tilde{B}$ are:

$$\tilde{A} = \begin{pmatrix} u & \rho & 0 & 0 \\ 0 & u & 0 & 1/\rho \\ 0 & 0 & u & 0 \\ 0 & \gamma p & 0 & u \end{pmatrix} \qquad \tilde{B} = \begin{pmatrix} v & 0 & \rho & 0 \\ 0 & v & 0 & 0 \\ 0 & 0 & v & 1/\rho \\ 0 & 0 & \gamma p & v \end{pmatrix} \tag{9}$$

The vectors V_{xx}, V_{xy}, V_{yx} and V_{yy} are as given in Eqn. 3.

We now non-dimensionalize these equations by reference values of the velocity, density, pressure, and temperature which will be denoted by a subscript R, and by a reference length L. Of particular interest is the momentum equation, and here we consider only the x-component. In non-dimensional form it becomes:

$$\frac{\partial u}{\partial \tau} + u \frac{\partial u}{\partial X} + \frac{p_R}{\rho_R u^2_R} \frac{1}{\rho} \frac{\partial p}{\partial X} + v \frac{\partial u}{\partial Y} = \frac{1}{\rho Re}(V.T.) \tag{10}$$

where the viscous terms (V.T.) are identical in form to those in Eqn. 8. The ratio of reference quantities that multiplies the pressure gradient can be expressed in terms of a reference Mach number,

$$\frac{\rho_R u_R^2}{p_R} = \gamma M_R^2 \tag{11}$$

where γ is the ratio of specific heats.

Because we are interested in flows where M_R is small, we define a small parameter, ε, as,

$$\varepsilon = \gamma M_R^2 \tag{12}$$

and expand all parameters in a power series in ε, as,

$$p = p_0 + \varepsilon p_1 + \ldots \tag{13}$$

Inspection of the non-dimensionalized equations shows that this substitution affects only the momentum and energy equations. The $1/\varepsilon$ multiplying the pressure gradient in the momentum equation implies the zeroeth order pressure must satisfy the relation:

$$\text{grad } p_0 = 0 \tag{14}$$

This indicates p_0 is a function of time only. For steady state problems we can, with complete generality, choose p_0 as a constant.

Using Eqn. 14 in the energy equation gives, after minor manipulation, the following low Mach number viscous system:

$$\begin{aligned}
&\frac{\partial \rho}{\partial t} + \frac{\partial}{\partial x}\rho u + \frac{\partial}{\partial y}\rho v = 0 \\
&\frac{\partial u}{\partial t} + u\frac{\partial u}{\partial x} + \frac{1}{\rho}\frac{\partial p_1}{\partial x} + v\frac{\partial u}{\partial y} = \frac{1}{\rho Re}(V.T.) \\
&\frac{\partial v}{\partial t} + u\frac{\partial v}{\partial x} + v\frac{\partial v}{\partial y} + \frac{1}{\rho}\frac{\partial p_1}{\partial y} = \frac{1}{\rho Re}(V.T.) \\
&\frac{\partial T}{\partial t} + u\frac{\partial T}{\partial x} + v\frac{\partial T}{\partial y} = \frac{1}{\rho RePr}\left(\frac{\partial^2 T}{\partial x^2} + \frac{\partial^2 T}{\partial y^2}\right)
\end{aligned} \tag{15}$$

where V.T. represents the appropriate viscous terms as given in Eqn. 3, and Re and Pr are the Reynolds and Prandtl numbers based on reference quantities. For simplicity, we have dropped the zero subscript on all variables in Eqn. 15 because the perturbation expansion causes only p_1 to appear.

Inspection of the coupled system, Eqn. 15, shows that there are five unknowns, ρ, u, v, T, and p_1, appearing. The density and temperature are related by the perfect gas law which, upon expansion, reduces to $p_0 = \rho T$. The problem with Eqn. 15 is that the time derivatives contain relations for both ρ and T along with u and v but there is no provision for updating p_1.

To circumvent this problem, we replace the time derivative in the continuity equation by an artificial time derivative as originally suggested by Chorin[13] for incompressible flow. Specifically, we replace the continuity equation in Eqn. 15 by,

$$\frac{\rho}{p_o}\frac{\partial p_1/\beta}{\partial t} + \frac{\partial \rho u}{\partial x} + \frac{\partial \rho v}{\partial y} = 0 \tag{16}$$

where β is a constant used for scaling. With this form of the continuity equation, the low Mach number system now contains p_1, u, v, and T in the time derivative. The simplified perfect gas relation immediately gives the density. Also, we note that the final three equations appear well-suited for viscous effects since they are all of the form:

$$\frac{\partial \phi}{\partial t} + \text{C.T.} = \nabla^2\phi \tag{17}$$

where ϕ represents u, v and T, respectively, and C.T. stands for convective terms.

To place Eqn. 15 into a form suitable for computation, we express it in conservation form using Eqn. 16 as the continuity equation. Upon combining these we obtain:

$$\Gamma\frac{\partial Q'}{\partial t} + \frac{\partial E'}{\partial x} + \frac{\partial F'}{\partial y} = \text{V.T.} \tag{18}$$

where,

$$\Gamma = \begin{pmatrix} \frac{\rho}{p_o} & 0 & 0 & 0 \\ \frac{\rho u}{p_o} & \rho & 0 & 0 \\ \frac{\rho v}{p_o} & 0 & \rho & 0 \\ 1 & 0 & 0 & \rho \end{pmatrix} \tag{19}$$

β = beta; ϕ = phi; ∇ = nabla; Γ = gamma

and

$$Q' = (p_1/\beta,\ u,\ v,\ T)^T$$
$$E' = (\rho u,\ \rho u^2+p_1,\ \rho uv,\ \rho uT)^T \qquad (20)$$
$$F' = (\rho v,\ \rho uv,\ \rho v^2+p_1,\ \rho vT)^T$$

CONVERGENCE OF LOW MACH NUMBER SYSTEM IN INVISCID FLOW

To test the perturbed low Mach number formulation we first apply it in inviscid flow. Convergence of an implicit scheme is closely related to the eigenvalues of the flux Jacobians. For this low Mach number system, the eigenvalues are:

$$\lambda(\Gamma^{-1}A') = (u,\ u,\ (u+c')/2,\ (u-c')/2) \qquad (21)$$

where $A' = \partial E'/\partial Q'$, and

$$c'^2 = u^2 + 4\beta T \qquad (22)$$

In order to get well-conditioned eigenvalues, we choose β as unity. Consequently, the flow described by Eqn. 18 is always "subsonic", an outcome in keeping with our physical expectations.

Convergence results for the inviscid model problem of Fig. 1 based on the low Mach number equations are given in Fig. 4 for a Mach number of 10^{-3}. Identical rates of convergence are obtained at Mach numbers of 10^{-1} and 10^{-5}. The expansion has completely removed the dependence on Mach number. The convergence observed with the complete equations at the high subsonic speed is observed with the low Mach number equations at all speeds.

λ = lambda

CONVERGENCE IN LOW MACH NUMBER VISCOUS FLOWS

To test the capability of the present low Mach number expansion in viscous flows, we again use the physical problem in Fig. 1, but with no-slip conditions enforced at the wall. Representative convergence rates obtained at several different Reynolds numbers are shown in Fig. 5. These results are all for a Mach number of 10^{-3}. At high Reynolds numbers where the viscous terms are small, they have little or no effect on convergence. As shown on the Figure, the rate of convergence at a Reynolds number of 1000 is nearly the same as for the inviscid case. (In fact, the effect of viscosity at these high Reynolds numbers is to make the rate of convergence modestly faster than in the inviscid case. This is because the physical diffusion serves to dissipate the errors in the solution slightly more rapidly.) By contrast, the rate of convergence at low Reynolds numbers is much slower than in the inviscid case. The case at a Reynolds number of 10 in Fig. 5 is seen to converge at about one-fourth the rate of the inviscid case. Flowfields at Reynolds numbers less than 10 failed to converge entirely. The reasons for this slowdown in convergence at low Reynolds numbers are again best demonstrated by investigating the stability characteristics of the low Mach number equations.

Figure 6 shows the stability characteristics of the low Mach number for the three Reynolds number cases discussed in Fig. 5. At a Reynolds number of 1000, the stability results are slightly more favorable than for the inviscid case thereby justifying the relative convergence rates for the two conditions. Values over much of the wavenumber domain range between 0.90 and 0.95. At a Reynolds number of 10, the amplification

factors remain stable, but are very near unity in all wavenumber regimes. Typical values here are above 0.98. These larger amplification ratios explain the slow convergence that was observed at Re=10.

The reason for this increase in amplification factor can be understood by recalling that the CFL condition of inviscid flow is joined by a second dimensionless quantity in viscous flows that is here referred to as a von Neumann number, $\sigma = \Delta t/(Re\ \Delta x^2)$. The slowdown in convergence at low Reynolds numbers is because the von Neumann number becomes large and the approximate factorization error in the diffusive terms drives the amplification factor toward unity and slows convergence. For inviscid flow, the von Neumann numbers are zero. At a Reynolds number of 1000, they are $\sigma \simeq 0.25$, while at Re = 10, σ has increased to 24. Rapid convergence requires that both the CFL and the von Neumann numbers be of order unity.

The most obvious way to control both the Courant and the von Neumann numbers simultaneously is by changing the grid size. Figure 7 shows stability results for Re=0.1 (which is a worse case than those on Fig. 6c) with the grid spacing being increased to give $\sigma = 3.8$ while CFL has been fixed at 8. These values of parameters provide amplification factors that are considerably farther from one, and promise much faster convergence than do the stability characteristics on Fig. 6c. Unfortunately, the grid size required to attain this value of σ is larger than the computational domain and so has no practical utility. The perturbation expansion does, however, give us an alternative method for fixing both non-dimensional parameters that is just as effective, but that does not require a change in the number of grid points. The method for achieving this is described in the next section.

σ = sigma; $\simeq$ = equals approximately

CONVERGENCE CONTROL AT LOW REYNOLDS NUMBER

For the viscous flow computations shown above, the scaling parameter β in the time derivative of the continuity equation was set to unity to provide properly scaled eigenvalues for the inviscid terms. As the Reynolds number is lowered, the inviscid terms become less important and the viscous terms begin to dominate. At these low Reynolds number conditions, it is no longer preferable to select β to provide properly scaled eigenvalues for the inviscid terms. Instead, we can use the parameter β to enable us to specify both the von Neumann number and CFL.

In the inviscid limit we pick the step size, Δt, by an appropriate CFL number,

$$CFL = \frac{(u+c')\Delta t}{2\Delta x} \tag{23}$$

whereas in the viscous limit the appropriate grouping of the time step is the von Neumann number,

$$\sigma = \frac{\Delta t}{Re\Delta x^2} \tag{24}$$

By solving Eqns. 23 and 24 for Δt and equating, we find,

$$\Delta t = \frac{2CFL\Delta x}{(u+c')} = \sigma Re\Delta x^2 \tag{25}$$

Inserting the definition of c' from Eqn. 22, and solving for β gives,

$$\beta = \frac{u^2}{4T}\left\{\left(\frac{2CFL}{\sigma Re_{\Delta x} u} - 1\right)^2 - 1\right\} \tag{26}$$

where $Re_{\Delta x}$ is the cell Reynolds number, $\rho_R u_R \Delta x/\mu_R$. Note that both u and T are non-dimensional and so are of order one.

With this expression, we can now specify both the von Neumann number and the Courant number and then use Eqn. 26 to compute β. Knowing β we can then compute Δt from Eqn. 25 and proceed to the numerical solution. Choosing σ=3.8, CFL=8 and computing β in this fashion brings the stability results of Fig. 6c to values shown in Fig. 8. This stability map is almost identical to the one shown on Fig. 7 that was obtained by changing Δx, and again promises fast convergence. The value of β required to obtain the results on Fig. 8 is β = 100.

For a wide range of Reynolds numbers, we therefore recommend that the parameter β be chosen according to the relation:

$$\beta = \text{Max}\left\{1, \frac{1}{4}\left[\left(\frac{2CFL}{\sigma Re_{\Delta x}} - 1\right)^2 - 1\right]\right\} \qquad (27)$$

where we have dropped the order one terms from Eqn. 26. This function is plotted as a function of the cell Reynolds number in Fig. 9.

Rates of convergence for several values of Reynolds number using the value of β given in Fig. 9 are shown in Fig. 10. With β defined as in Eqn. 27, the rate of convergence of the low Mach number system remains almost unchanged for Reynolds numbers ranging from infinity to 0.01. Clearly, this modification makes the time-iterative procedure much more robust.

LOW SPEED HEAT ADDITION AT VARIOUS REYNOLDS NUMBERS

To demonstrate the capability of the low Mach number/low Reynolds number formulation, we present flowfield results for the heat addition problem described in Fig. 1. A series of plots showing temperature and velocity contours for a fixed volumetric heat addition and an inlet Mach number of 1×10^{-5} are given in Fig. 11 for Reynolds numbers of infinity

(inviscid), 5000, 500, 50, and 0.05. The qualitative effects of viscosity are easily recognized in these plots. For inviscid flow the temperature contours are convected out of the flowfield with no diffusion, and the slip boundary condition shows no boundary layer on the wall in the velocity contour plot. At a Reynolds number of 5000, a modest diffusion of the temperature from the hot to the cold fluid is noted, and a thin boundary layer exists near the wall. Reducing the Reynolds number to 500 and then to 50 shows the increasing effects of heat diffusion and a thicker boundary layer as the effects of diffusivity spread over nearly the entire flowfield. Jumping to a Reynolds number of 0.05, the effects of convection are now completely absent in the temperature contours. The temperature contours give an undistorted image of the volumetric heat source. The velocity field at this low Reynolds number condition becomes nearly fully developed after the peak in the heat source is passed and shows no reminiscence of boundary layer flow. The value of β used for each case is given in the Figure.

Additional flowfield solutions showing the effect of heat addition through the walls are given in Fig. 12. Here, the temperature of the wall is linearly increased from T=1 at the inlet to T=6.67 at the exit, and the flow is heated through the boundary layer. In the inviscid case the flow is not affected by wall temperature and only viscous results are shown. At a Reynolds number of 5000, both temperature and velocity contours show thin boundary layers near the wall. The temperature in the middle of the duct is unaffected by heating. At a Reynolds number of 50, the boundary layers are much thicker and the heat has diffused to the middle of the duct. At a Reynolds number of 0.05, the diffusion rates are high enough relative to the convective speed that the temperature is

uniform in y. The monotonic increase in temperature, however, causes the flow on the centerline to continue to accelerate.

This spectrum of flow conditions ranging from inviscid to viscous-dominated flow shows that the modified equations provide qualitatively correct variations in the velocity and temperature fields as the magnitude of the Reynolds number is varied. The fact that all calculations were obtained with the same algorithm and that all showed nearly identical rates of convergence is an indication of the broad capabilities of the approximately factored, implicit time-dependent algorithm when proper mathematics and physics are incorporated.

DISCUSSION AND CONCLUSIONS

Time-marching algorithms are widely used for the solution of transonic and supersonic flows and for problems containing embedded shock waves. These methods are equally applicable to inviscid and high-Reynolds-number viscous calculations. The algorithms provide accurate, efficient solutions in inviscid flows because they treat the convective terms appropriately. The addition of weak (high Reynolds number) viscous effects to this properly formulated inviscid procedure has little or no effect on convergence because the convective terms still dominate the flow. The convergence rate of the algorithm, however, becomes notoriously slow in regions where the Mach number is low. Experience at very low Reynolds number conditions is very limited (largely because of problems with the convective terms), but all evidence suggests a similar slowdown in convergence at low Reynolds numbers.

These limitations can seriously impair convergence rates in high speed flows because of local low speed regions adjacent to stagnation points or because of near wall, low Reynolds number effects in boundary

layers. Further, the limitation to high speed flows precludes computations of important new low speed problems such as combustion applications in which the strong heat addition requires the use of a compressible formulation even though the Mach numbers would suggest incompressibility. The purpose of the present paper has been to identify and remove these limitations on convergence so the time-marching procedure can be applied over a much broader regime.

Although previous papers have studied the inviscid low Mach number problem, none have considered the viscous problem. Simple computational experiments show that neither previous preconditioning procedures nor previous perturbation expansion procedures provide approaches that are effective in viscous flows. Accordingly, a new low Mach number expansion procedure was developed from the non-conservative equations that is applicable to both viscous and inviscid conditions. This expansion procedure provides a mechanism for properly scaling the eigenvalues of the convective terms thus ensuring fast convergence in inviscid flows at all Mach numbers. It also provides a mechanism for keeping both the von Neumann number and the Courant number of order one at very viscous conditions, thereby ensuring rapid convergence at low Reynolds numbers.

The resulting domain of convergence of the low Mach number, low Reynolds number procedure is summarized on Fig. 13. Rapid, effective convergence of the procedure is observed for Reynolds numbers ranging from infinity down to 0.05 and from Mach numbers between 0.3 and 10^{-6}. Rapid convergence is here defined as convergence rates within 20-30% of that obtained in inviscid flows at Mach 0.7. As indicated on the figure, the modified procedure gives slower convergence over a small corner of the Reynolds number/Mach number domain. For comparison, the much smaller

region of convergence of the original time-marching procedure for compressible flow is shown in the upper right-hand corner of the Re-Mach number domain. Clearly, the modified procedure based on the perturbation expansion makes the classical compressible algorithms much more robust over a much wider range of variables. In particular, this low Mach number procedure represents an effective numerical algorithm for the computation of low speed flows with strong heat addition.

ACKNOWLEDGEMENT

This work was sponsored by the Air Force Office of Scientific Research under Contract AFOSR 82-0196.

REFERENCES

1. Jones, L. W. and Keefer, D. R., "NASA's Laser-Propulsion Project", Astronautics & Aeronautics, Vol. 20, Sept. 1982, p. 66.

2. Shoji, J. M., "Potential of Advanced Solar Thermal Propulsion", Orbit-Raising and Maneuvering Propulsion: Research Status and Needs, Progress in Astronautics and Aeronautics, Vol. 89, 1984, pp. 30-47.

3. Briley, W. R., McDonald, H., and Shamroth, S. J., "A Low Mach Number Euler Formulation and Application to Time-Iterative LBI Scheme", AIAA Journal, Vol. 21, Oct. 1983, pp. 1467-1469.

4. Turkel, E., "Fast Solutions to the Steady State Compressible and Incompressible Fluid Dynamic Equations", ICASE Report No. 84-28, NASA CR-172416, June 1984.

5. Choi, D. and Merkle, C. L., "Application of Time-Iterative Schemes to Incompressible Flow", AIAA Journal, Vol. 23, Oct. 1985, pp. 1518-1524.

6. Guerra, J. and Gustafsson, B., "Numerical Method for Incompressible and Compressible Flow Problems with Smooth Solutions", Journal of Computational Physics, Vol. 63, April 1986, pp. 377-397.

7. Rawshaw, J. D., O'Rourke, P. J. and Stein, L. D., "Pressure Gradient Scaling Method for Fluid Flow with Nearly Uniform Pressure", Journal of Computational Physics, Vol. 58, 1985, pp. 361-376.

8. Merkle, C. L. and Choi, Y. H., "Computation of Low-Speed Flow with Heat Addition", AIAA Journal, Vol. 25, June 1987, pp. 831-838.

9. Majda, A. and Sethian, J., "The Derivation and Numerical Solution of the Equations for Zero Mach Number Combustion", Combust. Sci. and Tech., Vol. 42, 1985, pp. 185-205.

10. Choi, Y. H., "Computation of Low Mach Number Compressible Flow", Ph.D. Thesis in Mechanical Engineering, to be completed in 1988.

11. Briley, W. R. and McDonald, H., "On the Structure of Use of Linearized Block Implicit Schemes", Journal of Computational Physics, Vol. 34, 1980, pp. 54-77.

12. Warming, R. F. and Beam, R. M., "On the Construction and Application of Implicit Factored Schemes for Conservation Laws", SIAM-AMS Proceedings, Vol. 11, 1978, pp. 85-129.

13. Chorin, A. J., "A Numerical Method for Solving Incompressible Viscous Flow Problems", Journal of Computational Physics, Vol. 2, 1967, pp. 12-26.

LIST OF FIGURES

Fig. 11 Effects of volumetric heat addition on the flow through a duct for various Reynolds numbers. Inlet Mach number, 10^{-5}.

Fig. 12 Effects of wall heating on the flow through a duct for various Reynolds numbers. Inlet Mach number, 1×10^{-5}.

Fig. 13 Applicable flow regime of low Mach number viscous formulation in terms of Reynolds number and Mach number.

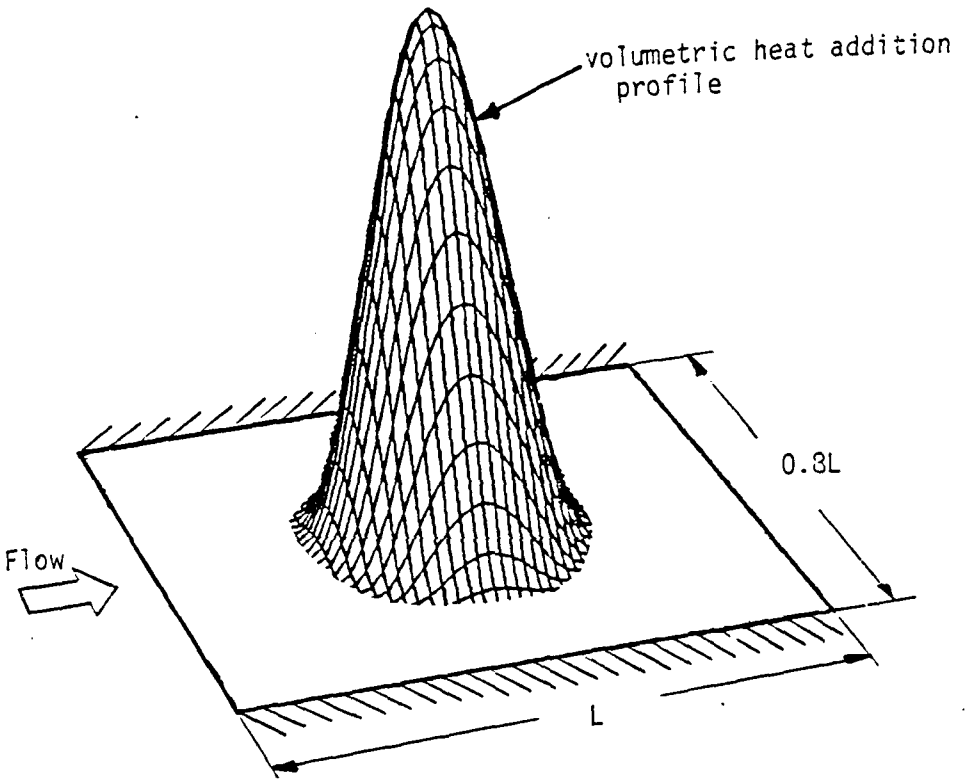

Figure 1

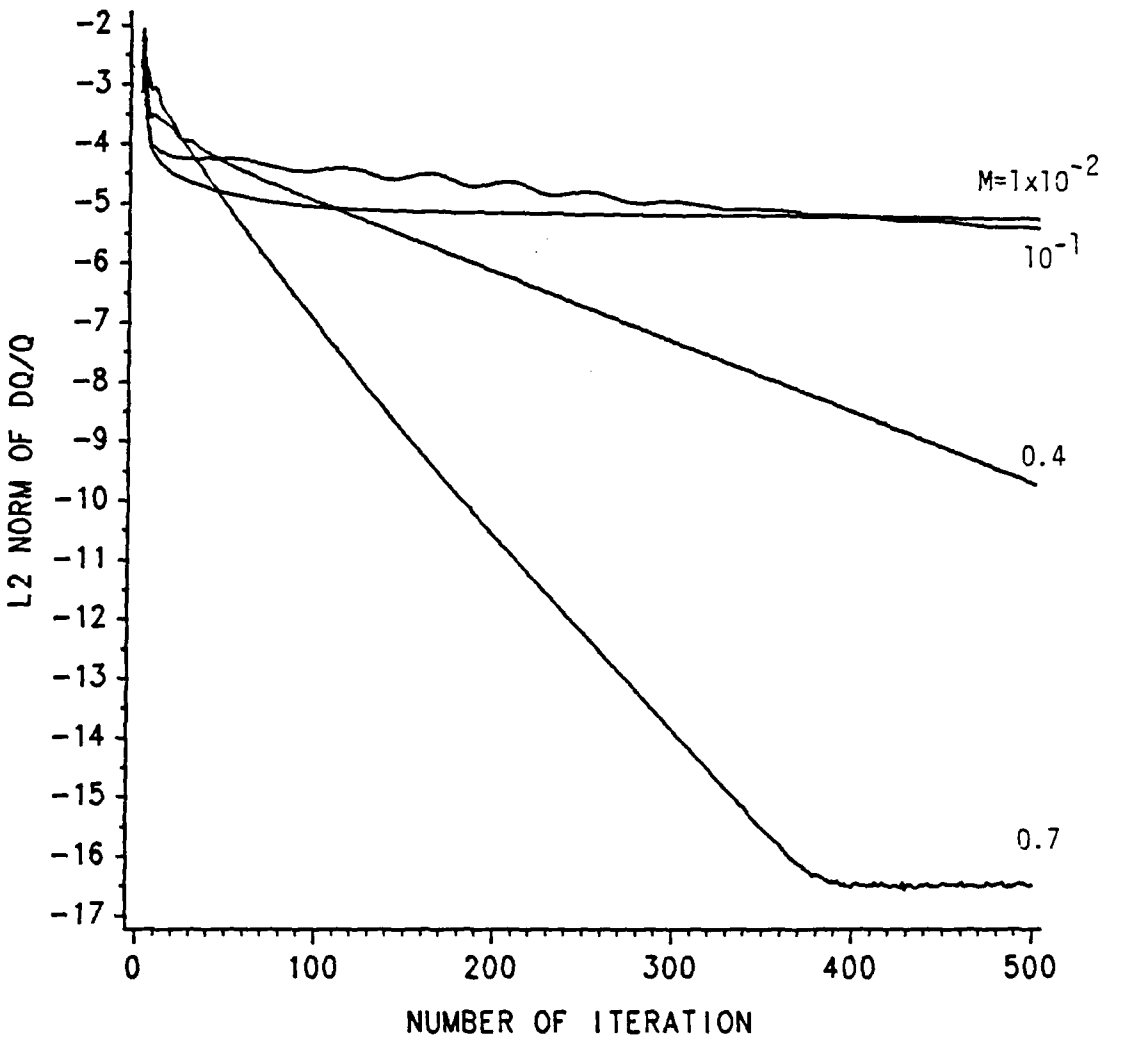
-2
-3
-4
-5
-6
-7
-8
-9
-10
-11
-12
-13
-14
-15
-16
-17
L2 NORM OF DQ/Q
0
100
200
300
400
500
NUMBER OF ITERATION
M=1x10^-2
10^-1
0.4
0.7

Figure 2

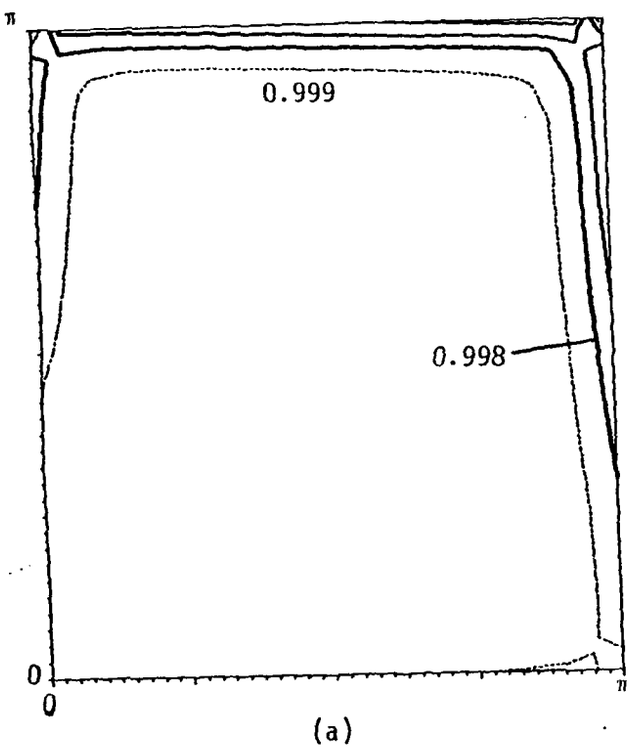

(a)

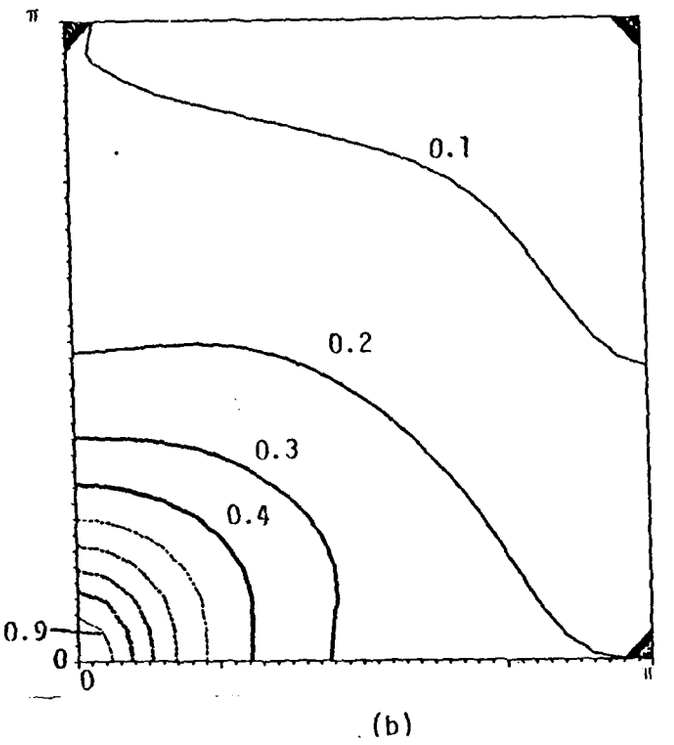

(b)

Figure 3

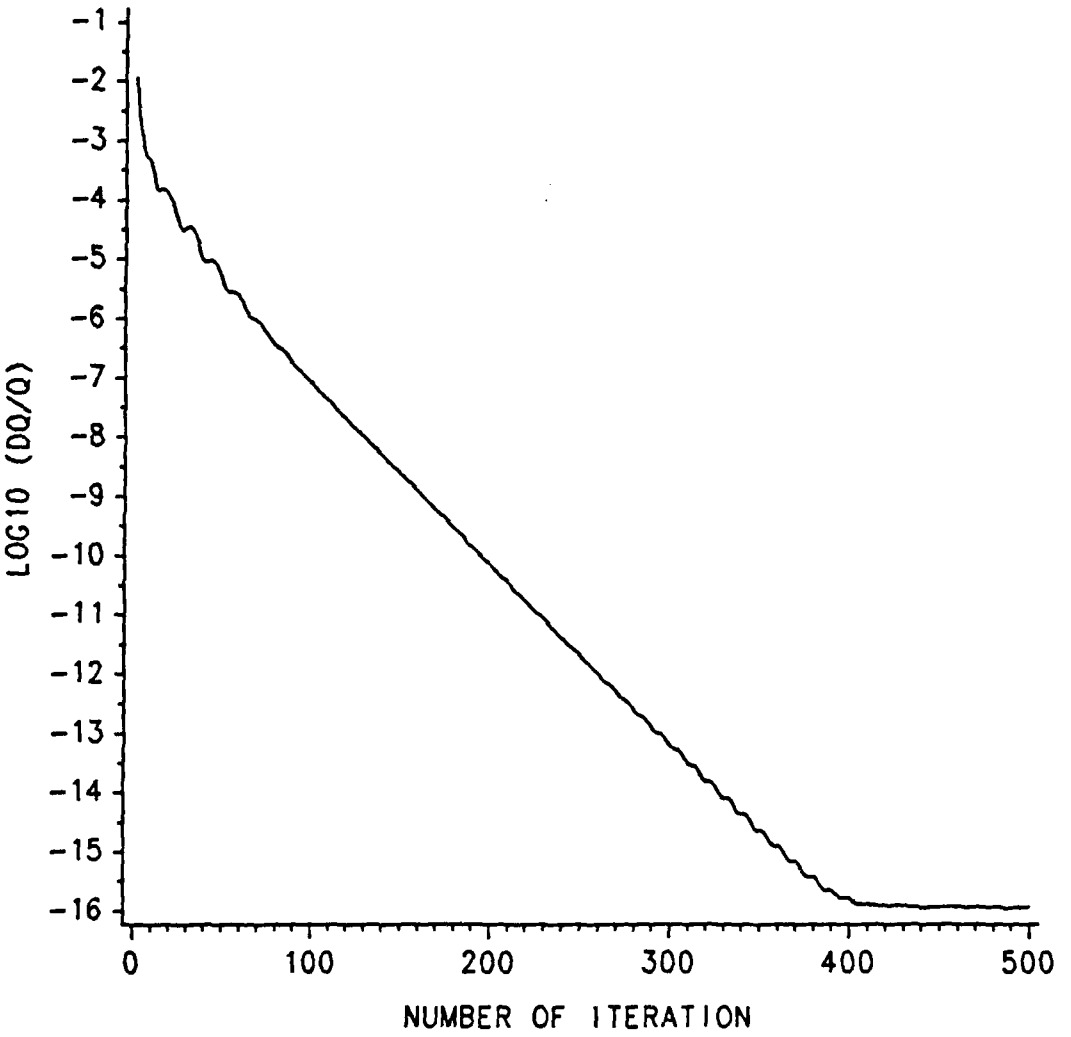
-1
-2
-3
-4
-5
-6
-7
-8
-9
-10
-11
-12
-13
-14
-15
-16
LOG10 (DQ/Q)
0
100
200
300
400
500
NUMBER OF ITERATION

Figure 4

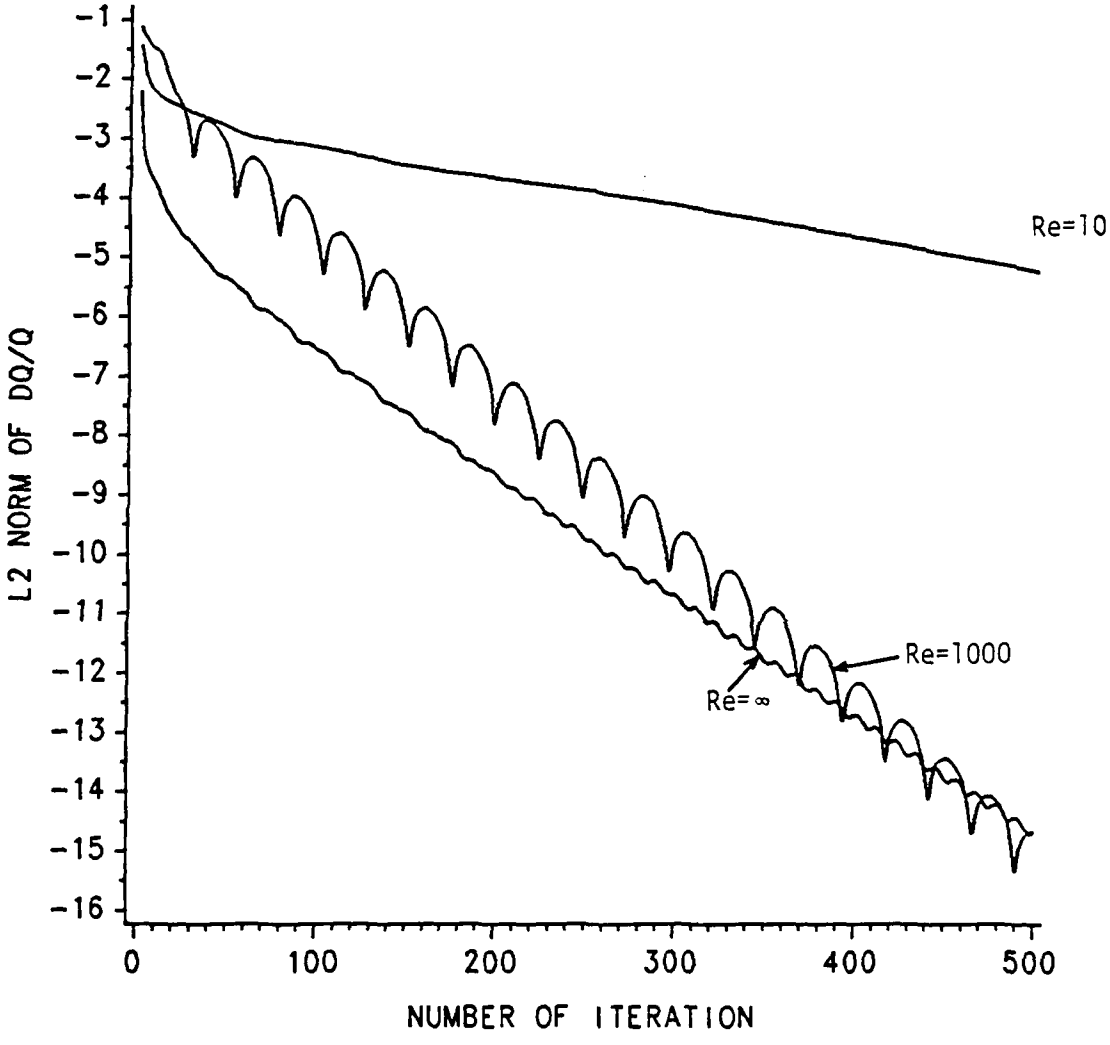
L2 NORM OF DQ/Q
-1
-2
-3
-4
-5
-6
-7
-8
-9
-10
-11
-12
-13
-14
-15
-16
0
100
200
300
400
500
NUMBER OF ITERATION
Re=10
Re=1000
Re=∞

Figure 5

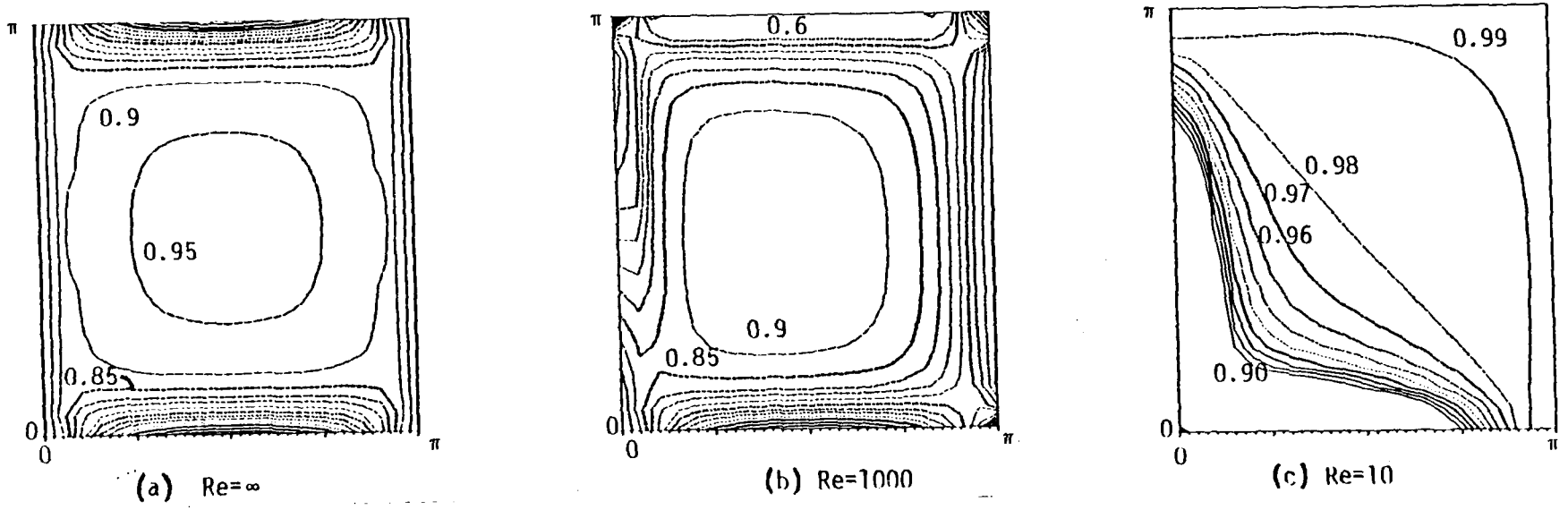
π
0.9
0.95
0.85
0
0
π
(a) Re=∞
π
0.6
0.9
0.85
0
0
π
(b) Re=1000
π
0.99
0.98
0.97
0.96
0.90
0
0
π
(c) Re=10

Figure 6

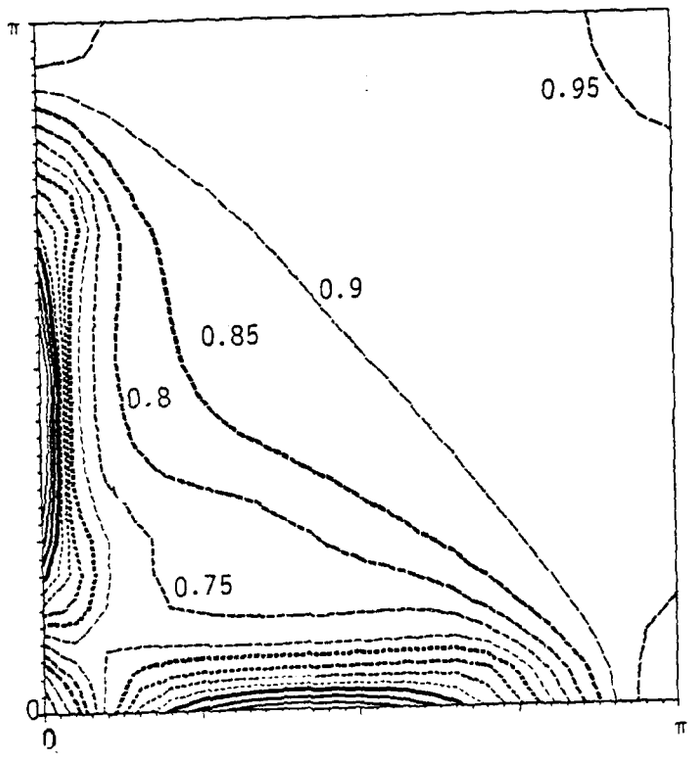

Figure 7

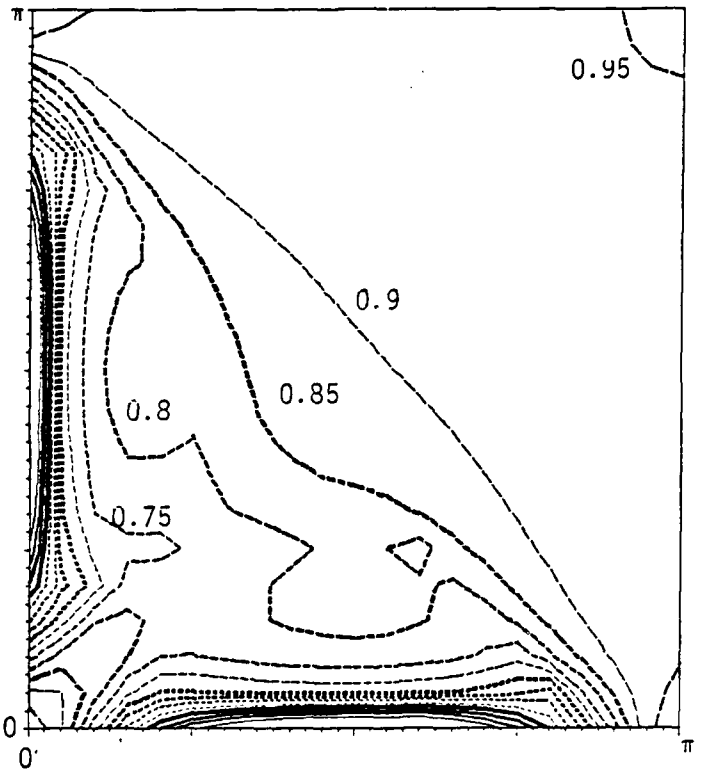

Figure 8

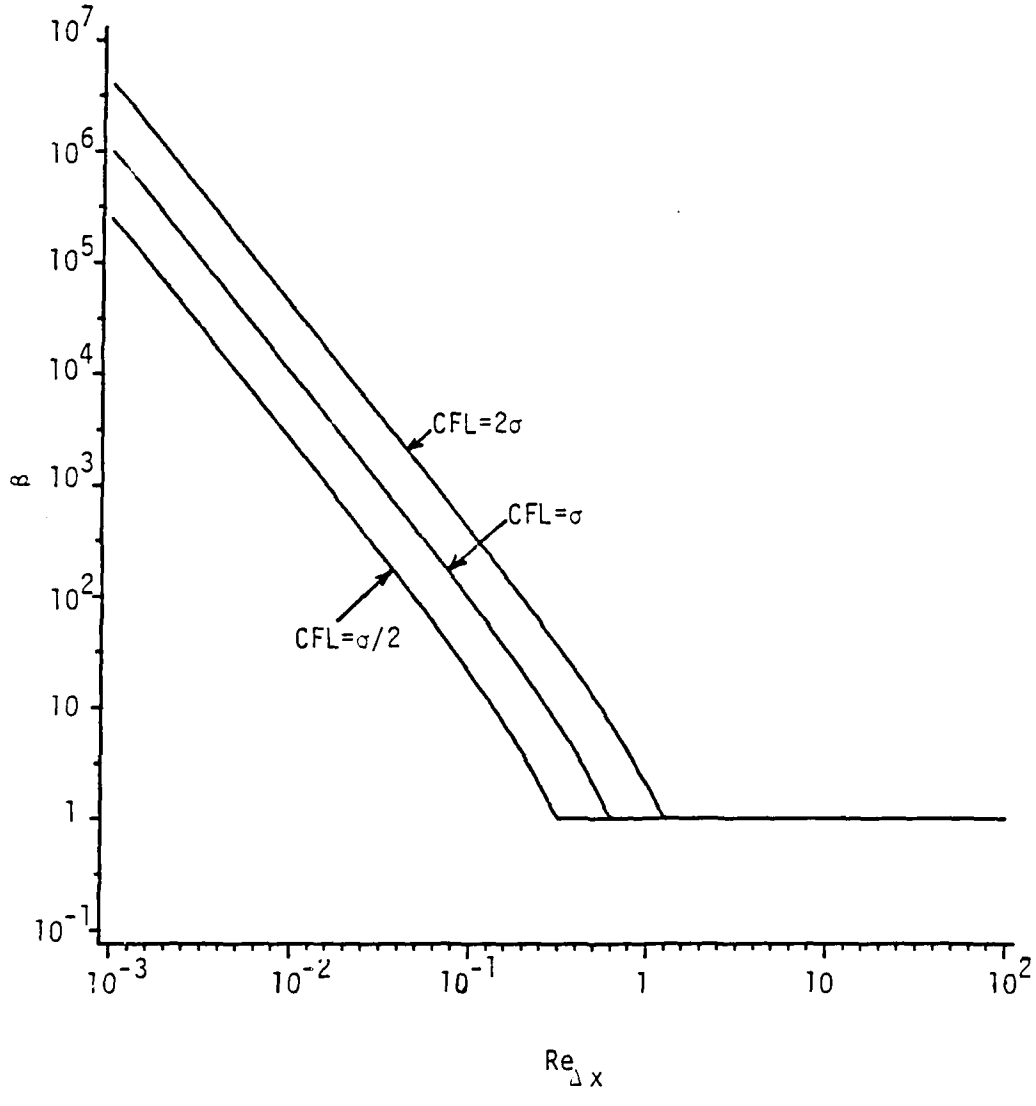
10^7
10^6
10^5
10^4
10^3
10^2
10
1
10^{-1}
β
CFL=2σ
CFL=σ
CFL=σ/2
10^{-3}
10^{-2}
10^{-1}
1
10
10^2
$Re_{\Delta x}$

Figure 9

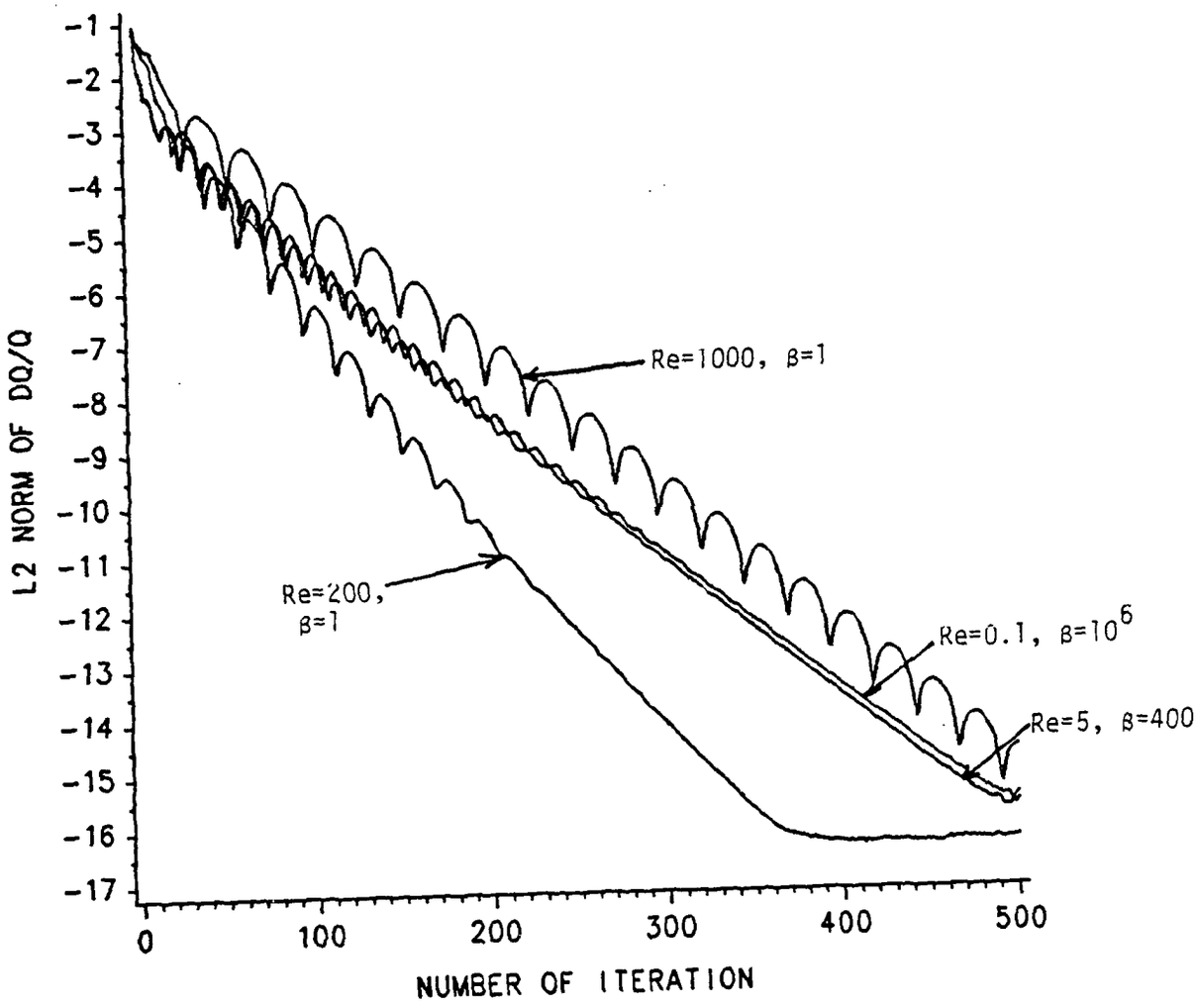
L2 NORM OF DQ/Q
-1
-2
-3
-4
-5
-6
-7
-8
-9
-10
-11
-12
-13
-14
-15
-16
-17
0
100
200
300
400
500
NUMBER OF ITERATION
Re=1000, β=1
Re=200, β=1
Re=0.1, β=10^6
Re=5, β=400

Figure 10

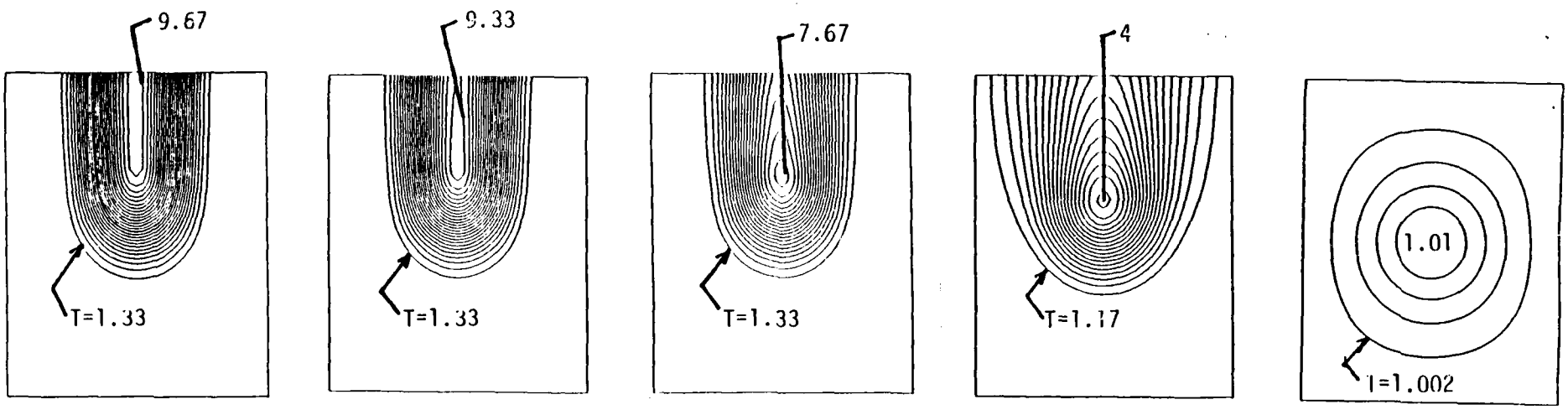

(a) Temperature Contours

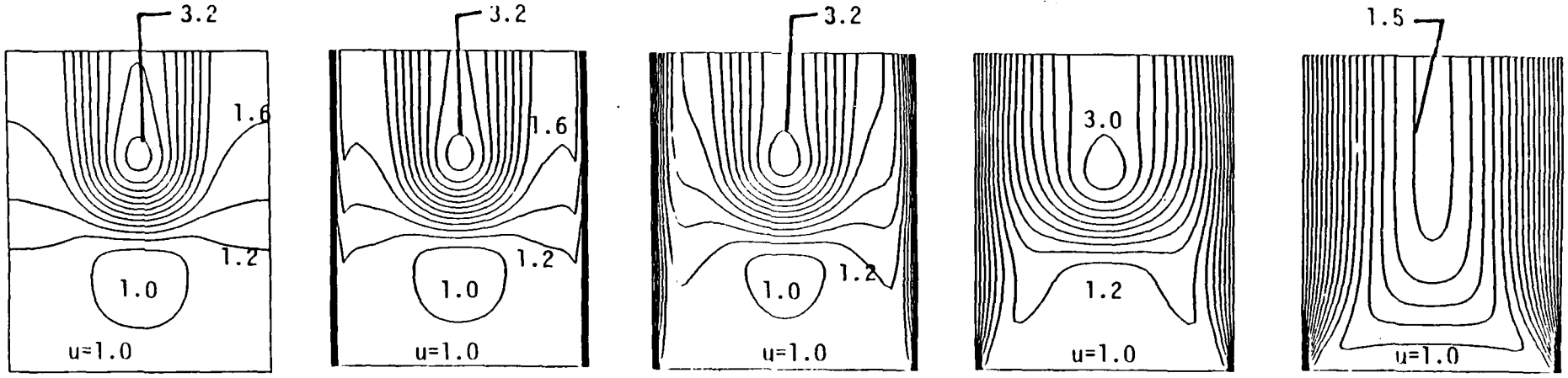

(b) Velocity Contours

Re=∞, β=1 | Re=5000, β=1 | Re=500, β=1 | Re=50, β=4 | Re=0.05, $\beta=4\times10^6$

Figure 11

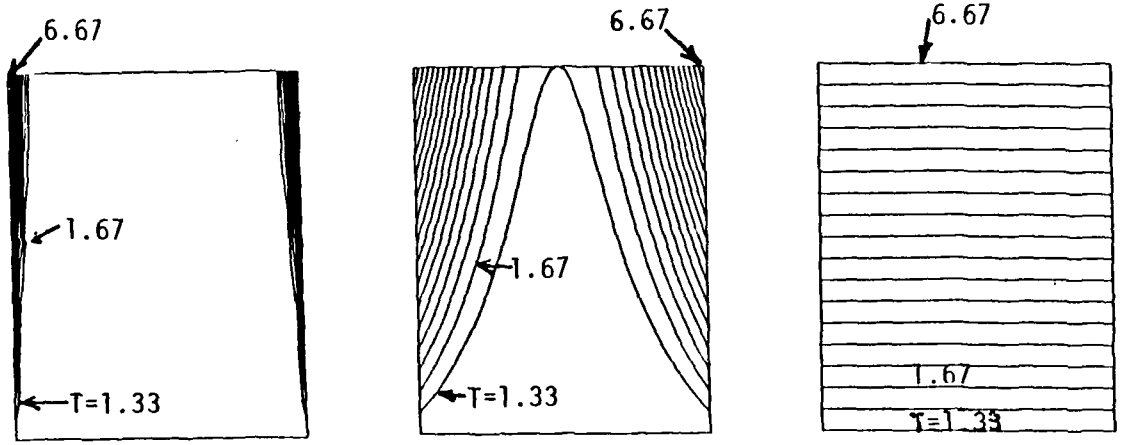

(a) Temperature

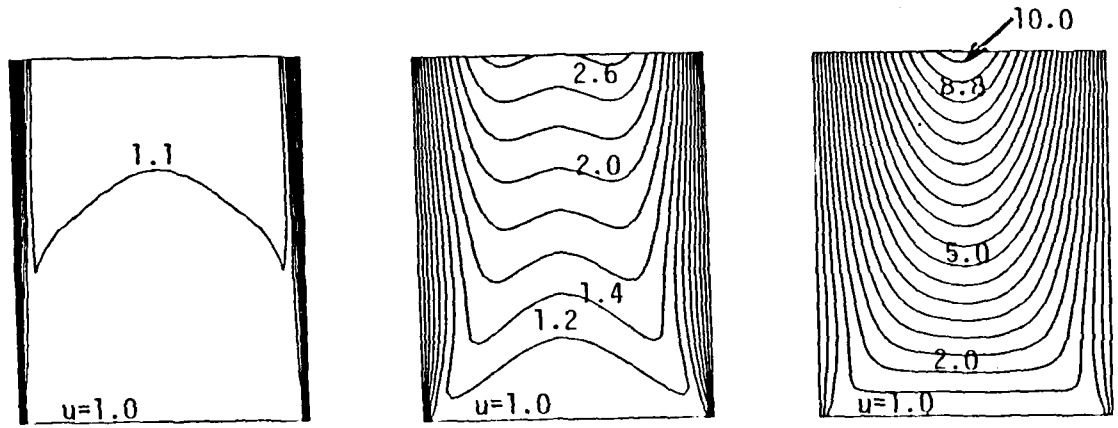

(b) Velocity

Re=5000, β=1

Re=50, β=4

Re=0.05, $\beta=4\times10^{6}$

Figure 12

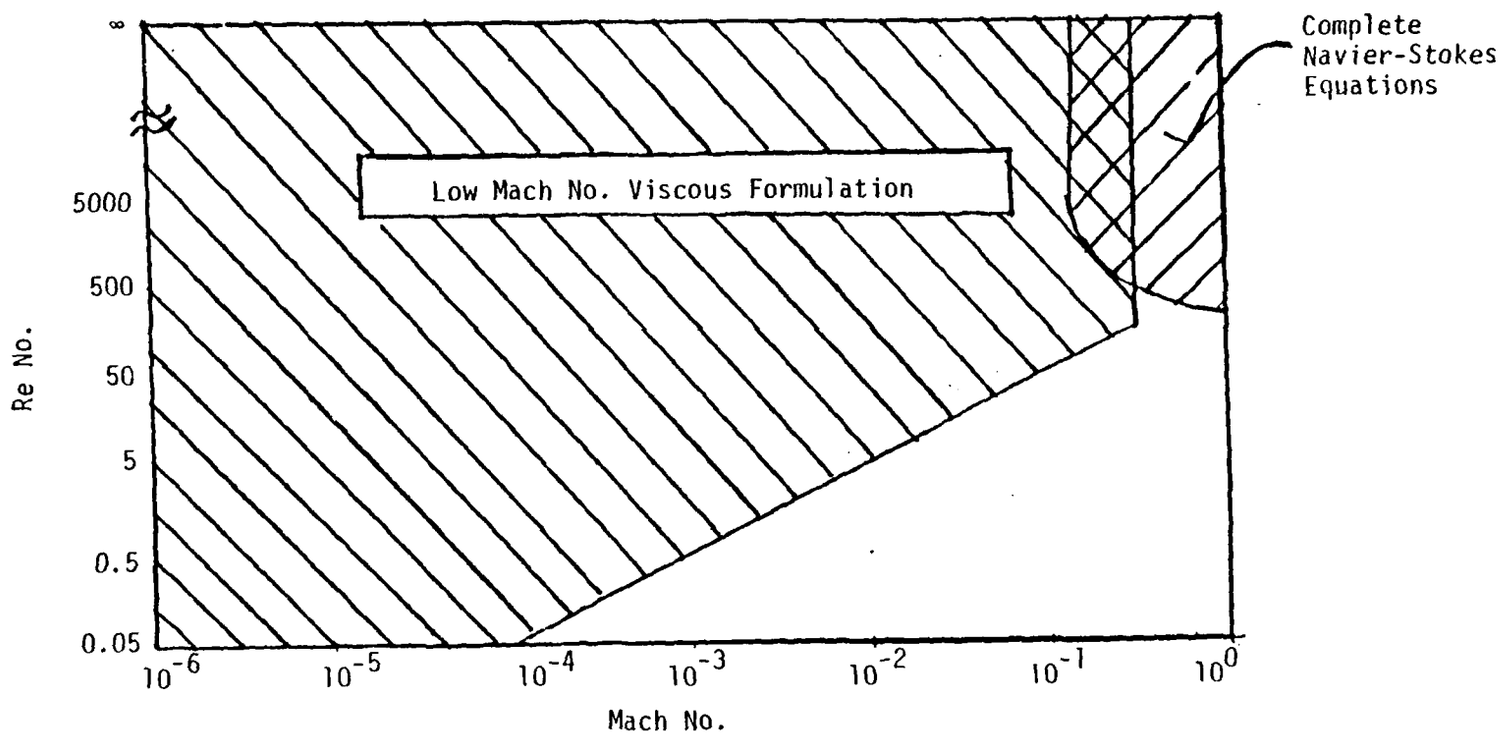
Complete
Navier-Stokes
Equations
Low Mach No. Viscous Formulation
∞
5000
500
50
5
0.5
0.05
Re No.
10^{-6}
10^{-5}
10^{-4}
10^{-3}
10^{-2}
10^{-1}
10^{0}
Mach No.

Figure 13